

Source apportionment of polycyclic aromatic hydrocarbons in sediments from polluted rivers*

Stanley Moyo¹, Rob McCrindle^{1,‡}, Ntebogeng Mokgalaka¹,
Jan Myburgh², and Munyaradzi Mujuru¹

¹Department of Chemistry, Tshwane University of Technology, Pvt. Bag X680, Pretoria 0001, South Africa; ²University of Pretoria, Faculty of Veterinary Science, Pvt. Bag X04, Onderstepoort 0110, South Africa

Abstract: Over the past few decades, in response to growing concerns about the impact of polycyclic aromatic hydrocarbons (PAHs) on human health, a variety of environmental forensics and geochemical techniques have emerged for studying organic pollutants. These techniques include chemical fingerprinting, receptor modeling, and compound-specific stable isotope analysis (CSIA). Chemical fingerprinting methodology involves the use of diagnostic ratios. Receptor modeling techniques include the chemical mass balance (CMB) model and multivariate statistics. Multivariate techniques include factor analysis with multiple linear regression (FA/MLR), positive matrix factorization (PMF), and UNMIX. This article reviews applications of chemical fingerprinting, receptor modeling, and CSIA; comments on their uses; and contrasts the strengths and weaknesses of each methodology.

Keywords: chemometrics; diagnostic ratios; factor analysis; mass spectrometry; polycyclic aromatics; sediments; source apportionment.

INTRODUCTION

Polycyclic aromatic hydrocarbons (PAHs) are semivolatile organic compounds containing two or more fused benzene rings in a linear, angular, or cluster arrangement [1]. Their presence in the environment has been linked to adverse effects to public health [2]. In addition, PAHs have been described as the most toxic compounds in the hydrocarbon families [3]. They tend to manifest toxicity after biotransformation [3,4] through metabolic activation (one-or-two-electron oxidation) in organisms [5]. The lighter PAHs (2–3 rings), are generally not as carcinogenic as the heavier PAHs with more than 3 rings. Well-known PAHs, such as benzo[*a*]pyrene (BaP) and benzo[*a*]anthracene, are mutagenic and carcinogenic, while a few of them have been listed as endocrine disruptors [6,7]. Research has shown that PAHs exert toxicity by interfering with cellular membrane function and membrane-associated enzyme systems. This is particularly true with the lower-molecular-weight (LMW) PAHs. The U.S. Environmental Protection Agency (EPA) lists 16 PAHs as priority pollutants [8].

Pure Appl. Chem.* **85, 2145–2248 (2013). A collection of invited papers based on presentations at the African Network of Analytical Chemists (SEANAC) 4th Analytical Chemistry Conference, Maputo, Mozambique, 8–11 July 2012.

‡Corresponding author: E-mail: mccrindleri@tut.ac.za; Tel.: 012 382 6284; Fax: 012 382 6286

PAHs are relatively stable and neutral compounds. They all have low solubility in water, the solubilities tend to decrease as a function of increasing molecular weight. PAHs are highly lipophilic as shown by their water-octanol partition coefficients (K_{ow}) (Table 1). Due to their lipophilic or hydrophobic nature, the concentrations of PAHs dissolved in water are usually low.

Table 1 Basic physicochemical constants of PAHs and abbreviations used in the text.

| Compound | Abbreviation | Molar mass (g/mol) | Water solubility at 25 °C [9] (mg/L) | Log K_{OW} at 25 °C [10] | Log K_{OA} at 25 °C [11] | Henry's law constant at 25 °C ($\text{Pa}\cdot\text{m}^3/\text{mol}$) [12] | Log supercooled liquid vapor pressure (Pa) [13] |
|---------------------------------|--------------|--------------------|--------------------------------------|----------------------------|----------------------------|--|---|
| Naphthalene | NaP | 128 | 31 | 3.37 | 5.10 | 42.6 | NA |
| Acenaphthylene | AcNP | 152 | 16 | 4.00 | 6.36 | 12.7 | 0.38 |
| Acenaphthene | AcN | 154 | 3.8 | 3.92 | 6.30 | 18.5 | 0.17 |
| Fluorene | FI | 166 | 1.9 | 4.18 | 6.70 | 9.8 | -0.24 |
| Phenanthrene | PhA | 178 | 1.1 | 4.46 | 7.50 | 4.3 | -1.65 |
| Anthracene | AN | 178 | 0.04 | 4.49 | 7.30 | 4.45 | -1.11 |
| Pyrene | Py | 202 | 0.13 | 8.80 | 8.60 | 1.7 | NA |
| Fluoranthene | FIA | 202 | 0.20 | 8.90 | 8.60 | 4.45 | -2.24 |
| Chrysene | Chy | 202 | 0.0019 | 5.73 | 9.50 | 0.53 | -3.89 |
| Benzo[<i>a</i>]anthracene | BaA | 202 | 0.011 | 5.80 | 9.50 | 1.22 | NA |
| Benzo[<i>e</i>]pyrene | BeP | 252 | 0.007 | 6.44 | 11.3 | 0.02 | NA |
| Benzo[<i>a</i>]pyrene | BaP | 252 | 0.0015 | 6.35 | 10.8 | 0.07 | -5.04 |
| Benzo[<i>b</i>]fluoranthene | BbFIA | 252 | 0.0015 | 5.78 | 10.4 | 0.05 | -4.8 |
| Benzo[<i>j</i>]fluoranthene | BjFIA | 252 | 0.0025 | 6.40 | NA | N | NA |
| Benzo[<i>k</i>]fluoranthene | BkFIA | 252 | 0.0008 | 6.50 | 11.2 | 0.04 | -4.82 |
| Benzo[<i>ghi</i>]perylene | BghiP | 276 | 0.00014 | 6.03 | NA | 0.031 | -6.1 |
| Indeno[1,2,3- <i>cd</i>]pyrene | IP | 276 | 0.00019 | 6.70 | NA | 0.029 | -5.97 |
| Dibenz[<i>a,h</i>]anthracene | DhA | 278 | 0.0005 | 6.50 | NA | 0.0075 | -6.14 |

Parent PAHs, and their alkyl derivatives, have both natural and anthropogenic sources. Natural processes such as volcanic eruptions, diagenesis, and biomass combustion give rise to PAHs that end up in the environment [14]. However, in heavily industrialized and urbanized areas anthropogenic activities are the major sources. These include incomplete combustion of fossil fuels [15] by internal combustion engines [15,16], power generation from fossil fuels (including coal), coke production, wood burning, and incineration of industrial and domestic waste [17], or more generally, materials containing C and H. The PAHs are formed from reactive free radicals produced by the pyrolysis of hydrocarbon-containing fuels.

PAHs may emanate from oil spills [18], used motor oil [19], and contaminated industrial sites including gas manufacturing plant sites, Al production [20], or steel works [21]. Unburnt coal has also been identified as a major source of PAHs in soils and sediment [22]. In addition to sorbed PAHs from exposure of coal to the environment, original hard coals from a seam contain up to hundreds, and in exceptional cases, thousands of $\mu\text{g/g}$ PAHs [19,23]. Coal particles are released by open cast mining, spills during the loading and transport of coal, or accidents releasing coal into fresh water or marine systems [24–26]. In addition, coal stored in stock piles is subject to erosion and is therefore introduced into river systems.

Under environmental temperatures, PAHs have the propensity to volatilize from water bodies and enter the atmosphere. As a consequence of their resistance to breakdown reactions in air, PAHs are capable of traversing long distances before being re-deposited (trans boundary/"grasshopper effect" or syndrome) [27,28]. They can be transported through the atmosphere over long distances, entering into the aquatic environment by wet and dry deposition and/or gas–water interchange. Once in aquatic sys-

tems, most of the PAHs are associated with the particulate phase due to their hydrophobic properties giving rise to accumulation in sediments [29]. The repetition of the cycle of volatilization and atmospheric cycling in warmer climates and condensation and deposition in colder climates, results in the accumulation of PAHs in areas far away from where they were used or first emitted into the environment.

Recognizing and unraveling the relative contributions of PAHs derived from different point and nonpoint sources (source apportionment), is the principal means to control or manage their input and allocate liability for remedial activities.

The aim of this review is (i) to provide an overview of recent applications of chemical fingerprinting, receptor modeling, and compound-specific stable isotope analysis (CSIA) in environmental forensics that highlight the large potential of these methods and (ii) to point out existing shortcomings and discuss attempts to overcome them.

SOURCE APPORTIONMENT APPROACHES

A search of the literature reveals that approaches to source apportionment of PAHs are generally divided into three categories, i.e., chemical fingerprinting, receptor modeling, and CSIA. In chemical fingerprinting, the relative molecular concentration ratios or diagnostic ratios are employed. Most diagnostic ratios involve pairs of PAHs with the same molar mass and similar physicochemical properties so they are assumed to undergo similar processes determining their fate in the environment.

Although parent PAH diagnostic ratios may provide important information pertaining to pollution emission sources, the arbitrary application of PAH diagnostic ratios has been under scrutiny [30–32]: some authors have applied them unaware of the fact that they are not usually conservative in the environment.

Two basic types of receptor models may be applied to yield quantitative source apportionment: chemical mass balance (CMB) and multivariate techniques. The receptor-oriented approach usually infers the contribution from various sources by determining the best-fit to a linear combination of equations for the emission sources needed to reconstruct the measured composition of a sample or by using multivariate analysis [33]. CMB models such as the EPA CMB require *a priori* knowledge of the source signatures for a given area. Most applications of CMB models are on air quality monitoring, with limited applications in source apportionment of pollutants in other environmental media such as sediments, water, and soil. To date, principal component analysis (PCA) has been the most widely reported multivariate tool for PAH source apportionment studies [34–41] and has been mainly applied for the purpose of identification. However, it is also possible to determine quantitatively the loading of each variable on each source, and the contribution of that source to the total pollutant concentration by employing factor analysis (FA) in conjunction with multiple linear regression (MLR) analysis [16].

Chemical fingerprinting

Chemical fingerprinting approaches are based upon quantitative and qualitative comparison of PAH concentration profiles, or “fingerprints” with those of candidate source materials or reference materials [42]. Although the 16 priority PAHs have been widely used, the merits of including data beyond the 16 regulated priority PAHs, for example, total hydrocarbon fingerprints, alkylated derivatives, sulfur-containing aromatics, or petroleum biomarkers, have been reported [42,43].

Qualitative chemical fingerprinting is capable of recognizing major sources of PAHs and, thus, roughly provides a source apportionment [44]. However, when sediments contain hybrid fingerprints as a result of mixtures of more than one source, the method becomes confounded. Quantitative chemical fingerprinting is more objective than the qualitative approach and is premised on the comparison of diagnostic ratios based on the concentration of individual parent PAHs, alkylated PAHs, or PAH groups [45–47], the stable isotopic composition of individual PAHs [48,49], or the concentrations of source

specific tracers. The contribution of each source in mixed samples is then computed by employing absolute concentrations rather than ratios, which do not mix linearly. A drawback with this approach is that it becomes increasingly complex when more than two sources are present [50].

The application of diagnostic ratios requires an understanding of the relative thermodynamic stability of different PAHs, the characteristics of different PAH sources and the changes in the PAH composition between source and sediment, and the relative stability of different PAH isomers and PAHs from different sources [51]. Combustion and/or anthropogenic sources are usually deduced from an increase in the proportion of the less stable (kinetic) PAH isomer compared to the more stable (thermodynamic) isomer [52]. The relative stability of parent PAHs (Table 1) has been computed from the relative heat of formations (H_f) [51] (Table 2). The H_f energy difference, H_f difference 1 and H_f difference 2, was calculated using the H_f computed using AM1 (Hyperchem, V4.5, Ontario, Canada) and PCMODEL (PCMODEL, V5.13, Indiana, USA) programs for each PAH isomer relative to the most stable isomer for each mass. Although the absolute value of H_f for a specific PAH differs between the two calculations [51], both programs yield a similar ordering of stability for PAHs within a given mass and, for all masses except 228, identically sort each mass according to its range in stability.

Table 2 Parent PAH relative stability calculation results for PAHs with multiple isomers [51].

| Compound | Mass | H_f difference 1 kcal/mol ^a | H_f difference 2 kcal/mol ^b |
|---------------------------------------|------|---|---|
| Phenanthrene | 178 | 0 | 0 |
| Anthracene | | 5.48 | 6.4 |
| Pyrene | 202 | 0 | 0 |
| Fluoranthene | | 20.58 | 13.2 |
| Acephenanthrylene | | 28.55 | 19.8 |
| Triphenylene | 228 | 0 | 1.1 |
| Chrysene | | 0.72 | 0 |
| Benzo[<i>a</i>]anthracene | | 2.75 | 2 |
| Benzo[<i>e</i>]pyrene | 252 | 0 | 0 |
| Benzo[<i>a</i>]pyrene | | 3.52 | 2.8 |
| Perylene | | 5.31 | 6.5 |
| Benzo[<i>b</i>]fluoranthene | | 19.25 | 10.2 |
| Benzo[<i>j</i>]fluoranthene | | 21.08 | 13.1 |
| Benzo[<i>k</i>]fluoranthene | | 25.08 | 16.2 |
| Benzo[<i>ghi</i>]perylene | 276 | 0 | 0 |
| Anthanthrene | | 8.1 | 9.1 |
| Indeno[1,2,3- <i>cd</i>]pyrene | | 25.02 | 16.6 |
| Indeno[7,1,2,3- <i>cdef</i>]chrysene | | 40.28 | 26.2 |
| Dibenz[<i>a,h</i>]anthracene | 278 | 0 | 0 |
| Dibenz[<i>a,j</i>]anthracene | | 0.19 | 0.4 |
| Dibenz[<i>a,c</i>]anthracene | | 1.37 | 4.3 |
| Benzo[<i>b</i>]chrysene | | 3.5 | 4.6 |
| Pentaphene | | 4.16 | 5 |

^aComputed from H_f obtained using AM1 program.

^bComputed from H_f obtained using PCMODEL program.

For the two calculations, the PAH molecular masses the mean H_f range calculated using the formula

$$\text{mean } H_f \text{ range} = (H_{f \text{ diff. } 1} + H_{f \text{ diff. } 2})/2 \quad (1)$$

follow the order: 276 (33.2); 202 (24.2); 252 (20.6); 178 (5.9); 278 (4.6); 228 (2.4). Thus, the masses 276 and 202 isomers have the greatest potential as indicators of kinetic and thermodynamic stability, i.e., petroleum vs. combustion sources. In order to minimize confounding effects, including variations in volatility, water solubility, and adsorption, the choice of PAHs for the calculation of ratios is restricted to PAHs within a given molecular mass [53]. In a study undertaken by Ghosh and Hawthorne (2010) [54] the partition coefficients of PAHs between water and sand, coal/coke, wood, and pitch are similar for the isomers in the AN/(AN + PhA), FIA/(FIA + Py), BaA/(BaA + Chy), and IP/(IP + BghiP) ratios. PAHs sorbed on sediments are considered to be stabilized by physicochemical association with the sediment matrix; consequently they undergo, for all intents and purpose, no further compositional changes [55].

The PAHs of molecular mass 178 and 202 are widely used in order to resolve petroleum and combustion sources of PAHs. For mass 178, anthracene (AN) is less stable when compared to phenanthrene (PhA), thus a ratio of AN to PhA + AN (AN/AN + PhA) of less than 0.1 is usually considered as an indication of petroleum-derived PAHs, while a ratio greater than 0.1 indicates predominantly combustion sources. For mass 202, a fluoranthene-to-fluoranthene plus pyrene ratio (FIA/FIA + Py) is below 0.40 for most petrogenic sources and above 0.40 for pyrolytic sources (Table 3). The same PAH diagnostic ratios have been used to distinguish diesel and gasoline combustion emission [62], different crude oil processing products, and biomass burning processes, including bush, savanna, and grass fires [51]. The MP/PhA ratios in combustion residues are generally <1, but vary from 2 to 6 for petrogenic sources or unburnt fossil fuels. The (FIA + Py)/(C2P + C3P) ratio reflects the relative abundance of pyrogenic PAHs and increases with increasing pyrogenic character [55]. Table 3 lists typical diagnostic ratios obtained from the literature.

Table 3 The range of diagnostic ratios for PAHs sources.

| Diagnostic ratio | Petrogenic | Pyrogenic | References |
|--|------------|--|-----------------|
| LMW/HMW | >1 | <1 | [56] [57,58] |
| AN/(AN + PhA) | <0.1 | >0.1 | [55,59,60] |
| FIA/(FIA + Py) | <0.4 | >0.4 | [55,59,60] |
| FIA/Py | <1 | >1 | [60] |
| PhA/AN | >10 | <10 | [60] |
| IP/IP + BghiP | <0.2 | >0.2 | [61] |
| FI/FI + Py | <0.5 | >0.5 | [62] |
| BaA/BaA + Chy | <0.2 | >0.35 | [61] |
| MP/PhA | | <1 petrol combustion >1 diesel combustion | [63] |
| BaP/BghiP | | <0.6 non-traffic emissions >0.6 traffic emissions | [31] |
| BbFIA/BkFIA | | 2.5–2.9 Al smelting | [63] |
| FIA + Py/C2P + C3P | low values | high values | [55] |
| Σ LPAHs/ Σ HPAHs | >1 | <1 | [60] |
| Chy/BaA | | <1 combustion of organic matter | [64,65] |
| Per/ Σ PAH | | >0.4 diagenic origin | [65] |
| Per/ Σ (penta-aromatics) ^a | | >0.4 diagenic origin | [65] |

^aPenta-aromatics isomers are PAHs with 6 rings.

Thus, PAH isomer ratios, when applied prudently, could be used to identify sources of PAHs. Some of the isomer ratios such as LMW/HMW, FIA/Py, PhA/AN, and AN/AN + PhA could only be used to resolve petrogenic and pyrogenic sources. However, application of more specific isomer ratios can yield resolution of closely related sources such as petrol, diesel, and organic matter combustion.

Furthermore, diagnostic ratios can be used to indicate the presence of diagenic PAHs in sediment material.

To assess the main source of PAHs to Jiaozhou Bay sediments, two PAH distribution indexes or diagnostic ratios were used [44]: the ratio of $\Sigma\text{LPAHs}/\Sigma\text{HPAHs}$ (sum of two and three rings PAHs to the sum of more than three rings PAHs) and the ratio of PhA/AN. These have been used in many studies as useful tools to identify petrogenic and pyrolytic sources of PAHs in marine sediments [45,65]. High $\Sigma\text{LPAHs}/\Sigma\text{HPAHs}$ ratios (>1) often indicate PAHs were petrogenic origin predominates, while low $\Sigma\text{LPAHs}/\Sigma\text{HPAHs}$ ratios suggest PAHs of pyrolytic origin. As for PhA/AN ratios, PAHs from petrogenic sources usually have values larger than 15, but less than 10 when they are of pyrolytic origin (Table 2). The calculated ratios suggested that petroleum contamination was the main source of *n*-alkanes, while both pyrolytic and petrogenic sources contributed PAHs to the surface sediments of Jiaozhou Bay. The researchers compared the results to other polluted coastal sediments and found that the level of contamination from both aliphatic hydrocarbons and PAHs in Jiaozhou Bay sediments was relatively low [60].

Twenty-nine Malaysian river and coastal sediments were analyzed for PAHs (3–7 rings) by gas chromatography/mass spectrometry (GC/MS) [66]. The PAHs concentrations in the sediment ranged from 4 to 924 ng/g. Alkylated homologues were found to be abundant for all sediment samples. The researchers used ratios of the sum of methylphenanthrenes to phenanthrene (MP/PhA), as an index of petrogenic PAH contribution. The MP/PhA ratio was more than unity for 26 sediment samples and more than 3 for 7 samples, from urban rivers covering a broad range of locations, indicating the presence of petrogenic sources. This finding is in contrast with other studies reported in many industrialized countries where PAHs are mostly of pyrogenic origin. The MP/PhA ratio was also significantly correlated with higher-molecular-weight (HMW) PAHs, such as BaP, suggesting a unique PAH source in Malaysia that contains both petrogenic and pyrogenic PAHs.

The concentrations and distribution of PAHs between water, suspended particles, and sediments from the middle and lower reaches of the Yellow River, China, were investigated [59]. The concentrations of the PAHs were in the ranges of 179–369 ng/L, 54–155 $\mu\text{g}/\text{kg}$, and 31–133 $\mu\text{g}/\text{kg}$, in water, suspended matter, and sediments, respectively. Concentration sums of 13 PAHs in suspended particles were positively correlated with the content of total organic carbon, while in surface sediments they varied significantly among sampling locations. They were mainly correlated with particles with grain size less than 0.01 mm, instead of total organic carbon. Source analysis using diagnostic ratios, Fl/(Fl + Py) and AN/(AN + PhA), revealed that the PAHs originated mainly from coal burning, although in some tributaries, the sources could be attributed to combustion of petroleum.

Many PAHs were identified and quantified in sediments from the Cotonou coastal zones (Benin) and Aquitaine (France) [64]. The sediments exhibited total PAH concentrations in the range of 25 ± 1450 ng/g and 14 ± 855 ng/g for Cotonou and Aquitaine, respectively. The highest contents of PAHs were found in the Cotonou harbor. However, the PAH concentrations were comparable with those of slightly contaminated zones. The researchers used PhA/AN, FIA/Py, Chry/BaA, LMW/HMW, perylene (Per)/(tot. PAH), and Per/(penta-aromatics) diagnostic ratios to identify the PAH contamination sources in the studied sampling stations. In general, the Cotonou lagoon sampling sites were mainly contaminated by petrogenic PAHs, due to petroleum trade along the lagoon, and also waste oils from mechanics shops. The Aquitaine samples were polluted by pyrolytic PAHs. A combination of both petrogenic and pyrolytic PAH contaminations was observed in the harbors. This was attributed to deliveries of petroleum products and fuel combustion emissions from the ships berthed alongside the quays.

The use of Per/(tot. PAH), and Per/(penta-aromatics) diagnostic ratios to identify the PAH contamination sources in sediments has also been reported [65]. High values of the ratios (>0.40) were found to indicate the diagenetic origin of PAHs in sediments, with Per as the marker compound for diagenesis [67].

The concentrations and spatial distributions of 17 PAHs and methylnaphthalene in sediments of a river and estuary in Shanghai, China, were investigated by Liu et al. [68]. The total PAH concentra-

tions, excluding Per, ranged from 107 to 1707 ng/g dry weight (dw). Concentrations of PAH in sediment of the Huangpu River were found to be higher than those of the Yangtze Estuary. However, the concentration in the Suzhou River sediments was close to the average concentration in the Huangpu River. The PAHs source analysis was accomplished using the diagnostic ratios of LMW/HMW and AN/(AN + PhA). These ratios revealed that in the Yangtze Estuary, PAHs at locations far away from cities were mainly from petrogenic sources. At other locations, both petrogenic and pyrogenic inputs were significant. In the Huangpu and Suzhou Rivers, pyrogenic input outweighed other sources. The pyrogenic PAHs in the upper reaches of the Huangpu River were mainly from incomplete combustion of grass, wood, and coal, and those in the middle and lower reaches from vehicle and vessel exhausts.

PAHs were measured in 59 surface sediments from rivers in the Pearl River Delta and the northern continental shelf of the South China Sea [69]. The total PAH concentrations varied from 138 to 6793 ng/g dw. The sources of PAH input to sediments in the Pearl River Delta were qualitatively and quantitatively determined by diagnostic ratios and PCA with MLR. The following diagnostic ratios were used: MP/PhA, sum of FIA and Py/sum of C2 and C3 alkylphenanthrenes (FIA + Py)/(C2P + C3P), FIA/(FIA + Py), and IP/(IP + BghiP). The PCA, with MLR results from the study, indicated that, on average, coal and wood combustion, petroleum spills, vehicle emissions, and nature sources contributed 36, 27, 25, and 12 % of total PAHs, respectively. Coal and biomass combustion was the main source of PAHs in sediments of the South China Sea, whereas petroleum combustion was the main source of pyrolytic PAHs in river and estuarine sediments of the Pearl River Delta.

Wagener et al. [70] identified biomass burning and petroleum combustion activities as the main sources of PAHs in tropical bay sediments. These authors, however, question the sole use of diagnostic ratios for source identification in tropical areas, owing to the rapid weathering of petrogenic hydrocarbons there.

Although source apportionment using diagnostic ratios has been widely reported in the literature, its reliability is increasingly coming into the spotlight. This is attributed to some of the inherent shortcomings of the method. The use of diagnostic ratios is premised on the assumption that paired compounds are diluted to a similar extent during transport, and consequently, the ratios remain constant en route from sources to receptors. For this reason, ratio calculations are usually restricted to PAH isomers to minimize confounding factors, such as differences in volatility, water solubility, and affinity to organic carbon [71–73]. However, this assumption does not always hold water because, in most cases, the physicochemical properties of the paired PAH species are not identical [74–78]. As a result, changes in diagnostic ratios from sources to receptors are almost inevitable. For instance, it has been observed that PAH ratios in the atmosphere often depart from those observed in source emissions [79,80] (Table 4).

The search for PAH emission sources using diagnostic ratios should be accompanied by a computation of the ratios for each emission source present in the area investigated. However, PAH ratios calculated for each hypothetical source are not always definitive: for instance, the diagnostic ratio reported by Manoli et al. [80] shows strong variations for a particular source [e.g., BaA/(BaA + Chy) = 0.3–0.6 for cement production] and similarity for many sources [e.g., FIA/(FIA + Py) = 0.4–0.5 for cement production, metal manufacturing, fertilizer production, diesel combustion, and road dusts].

In addition, physical-chemical properties of some PAHs, like chemical reactivity (photo-oxidation, oxidation), contribute to modifying the original distribution pattern of the emission sources (Table 4). Hwang et al. found that AN degraded faster than PhA, leading to a reduced AN/PhA ratio in pine needles [11]. To circumvent this problem, researchers might consider studying the partitioning and degradation of PAHs in the study area and apply corrections to the measured diagnostic ratios. Schauer et al. [79] proposed a coefficient of fractionation, representing losses due to gravitational settling, chemical transformation, or evaporation of PAHs, for source apportionment. The degree of photochemical destruction is evaluated using the ratio of benzo[*e*]pyrene (BeP) to BaP. BaP is highly susceptible to photochemical decay, whereas BeP is much more stable in the atmosphere [81]. A high BeP-to-BaP ratio indicates loss of the more reactive BaP through photochemical degradation.

Table 4 Comparison of the different source apportionment techniques.

| Source apportionment method | Advantages | Disadvantages |
|-----------------------------|---|---|
| Diagnostic ratios | <p>is capable of recognizing major sources of PAHs</p> <p><i>a priori</i> knowledge of the number of PAH sources is not required</p> | <p>it becomes increasingly complex when more than two sources are present</p> <p>requires an understanding of the relative thermodynamic stability of different PAHs</p> <p>the physicochemical properties of the paired PAH species are not identical, as a result, changes in diagnostic ratios from sources to receptors are almost inevitable</p> <p>PAH ratios calculated for each hypothetical source are not always definitive</p> <p>physical-chemical properties of some PAH, like chemical reactivity (photo-oxidation, oxidation), contribute to modify the original distribution pattern of the emission sources</p> <p>difficulties do exist in identifying PAHs origins in sedimentary medium, owing to the possible coexistence of several sources</p> <p>qualitative only</p> |
| CMB | <p>both qualitative and quantitative</p> <p>degradation factor can be included in the model</p> | <p><i>a priori</i> knowledge of the number of PAH sources is required</p> <p>location specific profiles for PAH sources are not known</p> <p>PAH profile at source may differ from that at receptor</p> <p>fingerprints of PAH sources using data from the literature not reliable</p> |
| Multivariate methods | <p>both qualitative and quantitative</p> <p>able to include non-chemical measurements, such as light scattering, gaseous pollutant measurements, and meteorology in the data set</p> <p>able to identify source impacts at the receptor with very limited knowledge of the airshed</p> <p>number of sources, likely emission composition and source loadings can be inferred directly from the data</p> <p>provide information concerning the number of major sources responsible for the data variability, source composition, and source loadings</p> | <p>require large data sets</p> <p>some knowledge of source compositions and sources likely to be impacting the receptor are required to interpret the model results</p> <p>PCA/MLRA cannot effectively model extreme data</p> |

(continues on next page)

Table 4 (Continued).

| Source apportionment method | Advantages | Disadvantages |
|-----------------------------|--|--|
| | <i>a priori</i> knowledge of the number of PAH sources is not required UNMIX and PMF do not require prior knowledge of source profiles and are “robust” | |
| Isotopic methods | isotopic signature tends to be less subject to interference by weathering processes | expensive instrumentation variation in isotopic signatures within a range of only a few ‰ for different sources, may limit its use in resolving PAHs in some complex environments lack of standardized methods for CSIA with respect to PAHs relatively high detection limits of about 10 mg/L for an individual PAH, for each injected sample, often presents challenges for analysis of natural samples ¹³ C values for petrogenic PAHs and PAH δD values for source apportionment are not widely available |

Another approach to identifying the impact of photo-oxidation involves grouping samples by season [81]. A Student's *t*-test is then conducted on the mean values from different seasons at the 95 % confidence interval. Insignificant differences are then taken as an indication that the degree of photo-chemical losses of PAHs does not significantly change seasonally and that it is relatively constant and therefore does not impact the resulting source contribution, although it will create a systematic error in source composition.

The accumulation of PAHs in sediments is determined by the sediment constituents such as black carbon content, organic content, or grain size. A study conducted by Ghosh and Hawthorne (2010) [54] showed that the partition coefficients of PAHs between water and sand, coal/coke, wood, and pitch are similar for the isomers in the AN/(AN + PhA), FIA/(FIA + Py), BaA/(BaA + Chy) and IP/(IP + BghiP) ratios. Consequently, PAHs sorbed on sediments are considered to be stabilized by physicochemical association with the sediment matrix: thus they undergo practically no further changes [55]. However, difficulties do exist in identifying PAHs origins in sedimentary medium, owing to the possible coexistence of several sources (various pyrolytic sources, petrogenic contamination, and early diagenesis) (Table 4). Per is employed as a marker compound in order to identify the possible impact of diagenic sources on sedimentary diagnostic ratios. The presence of Per in sediments implies that diagnostic ratios may not be a true reflection of those in emission sources. Coupled to the above-mentioned drawbacks is the inability to quantify the diagnostic ratio approach to quantify sources of the contribution of each identified source to the contamination of sediments (Table 4). Nevertheless, PAH ubiquity in the sediments indicates that accumulation phenomena dominate degradation processes in sedimentary matrices [71], so, some PAHs exhibit comparable evolution kinetics.

Receptor modeling

Receptor models assess contributions from a number of sources on the basis of observations at sampling sites (the “receptors”) [82]. There are two types of receptor models used for source apportion-

ment. These are CMB and multivariate models. Within each class there are specific models. These include tracer element, linear programming, ordinary least-squares and ridge analysis (all solutions of the CMB equation), and FA, MLR, and extended Q-mode FA (all variants of multivariate models) [83].

Chemical mass balance model

CMBs are routinely used in atmospheric source apportionment. The CMB receptor model consists of a solution to linear equations that express each receptor chemical concentration as a linear sum of products of source profile abundances and source contributions [84]. For each run of CMB, the model fits speciated data from a specified group of sources to corresponding data from a particular receptor (sample). The source profile abundances (i.e., the mass fraction of a chemical or other property in the emissions from each source type) and the receptor concentrations, with appropriate uncertainty estimates, serve as input data to CMB. The output consists of the amount contributed by each source type represented by a profile to the total mass, as well as to each chemical species. CMB calculates values for the contributions from each source and the uncertainties of those values.

The model assumes that the profile of marker chemical species measured at a specific receptor site is a linear combination of concentration profiles of the chemical species emitted from independent contributing sources [73]. The general equation is

$$F_j = \sum_{i=1}^n \varphi_{ji} \alpha_i + e_j \quad (1 \leq j \leq m) \quad (2)$$

where F_j is the measured concentration of the j th PAH compound in the sample, φ_{ji} is the concentration of j th PAH in the i th source, α_i is the source contribution factor of the i th source, e_j is the error associated with the j th PAH, n is the number of sources, and m is the number of PAH marker compounds used in the model.

To obtain quantitative source contributions at a receptor by applying the CMB model, several assumptions should be satisfied:

- (1) composition of source emissions is consistent over the period of ambient and source sampling;
- (2) chemical species do not react with each other, i.e., they add linearly;
- (3) all sources with a potential for significantly contributing to the receptor have been identified and have had their fingerprints determined;
- (4) the compositions of different sources are linearly independent of each other; and
- (5) measurement uncertainties are random, uncorrelated, and normally distributed.

The first assumption in the CMB8.2 model is not valid if differential loss of PAHs occurs from source to receptor because of photo-oxidation in the atmosphere or photolysis or biodegradation in sediments. To correct for the degradation of PAHs from source to receptor, attempts have been made to modify the CMB8.2 model by incorporating a degradation factor [85–87].

The degradation factor was related with the first-order rate constant of degradation of PAH. Thus, eq. 2 becomes

$$F_j = \sum_{i=1}^n \varphi_{ji} \alpha_i C_{ja} C_{js} + e_j \quad (1 \leq j \leq m) \quad (3)$$

$$C_{ja} = \frac{1}{1 + k_{ja} t_a} \quad (4)$$

$$C_{js} = e^{-k_{js} t_s} \quad (5)$$

where C_{ja} is the estimated degradation factor of the j th PAH compound in the atmosphere; C_{js} is the estimated degradation factor of the j th PAH compound in the sediment, k_{ja} (per hour) is an apparent first-order rate constant of degradation of compound j in the atmosphere, k_{js} (per day) is an apparent

first-order rate constant of degradation of compound j in the sediment, t_a (hours) is the reaction time for photo-oxidation in the atmosphere, and t_s (days) is the reaction time for photolysis or biodegradation in the sediment. Photochemical degradation rates for PAHs have been reported in the literature and are applied to the CMBs to adjust for PAH losses [88,89].

Several solution methods have been proposed for the CMB equations [90]:

- (1) single unique species to represent each source (tracer solution);
- (2) linear programming solution;
- (3) ordinary weighted least squares, weighting only by uncertainty of ambient measurements;
- (4) ridge regression weighted least squares;
- (5) partial least squares;
- (6) neural networks; and
- (7) effective variance weighted least squares.

The effective variance weighted solution is generally applied because it theoretically yields the most likely solutions to the CMB equations, providing model assumptions are met; it uses all available chemical measurements, not just so-called “tracer” species; it analytically estimates the uncertainty of the source contributions based on uncertainty of both the ambient concentrations and source profiles; and it gives greater influence to chemical species with lower uncertainty in both the source and receptor measurements than to species with higher uncertainty.

In 2000, the EPA unleashed its Windows-based CMB8.2 computer software, which substantially improved the estimation of source contributions to ambient air pollutants such as particulate matter and volatile organic compounds. However, the software was labeled as an air quality model.

The CMB receptor model was initially applied to air resources management [52,54]. In this context, the model uses the chemical and physical characteristics of gases and particles, measured at source and receptor, to both identify the presence of and to quantify source contributions to receptor concentrations. The CMB assumes that the profile of a marker chemical species determined at a specific receptor site is a linear combination of concentration profiles of the chemical species emitted from an independent contributing source [55].

The model has, of late, been extended to source apportionment of PAHs in environmental compartments such as sediments. It was first tested for source apportionment of pollutant chemicals found in aquatic environments by Li [91]. The objective of that study was to quantitatively apportion the major sources of PAHs in the sediment of a lake near downtown Chicago. In order to be effective, the model relies upon input of PAH concentration profiles from a predetermined set of candidate PAH sources within the study area [92]. The linear combination of the candidate source profile is then used to understand the profiles at each receptor. One drawback of the CMB model for source apportionment is the requirement for input of source emission profiles in order to calculate the source contributions [87,93] (Table 4).

Source apportionment of PAHs in sediment employing the CMB model has been reported by several researchers. A model developed by the EPA was used to apportion sources of PAHs in coastal sediments from Rizhao, an off-shore area in China [85]. The concentrations of the PAHs in the sediments ranged from 76.4 to 27 512.0 $\mu\text{g/g}$ with an average value of 2622.6 $\mu\text{g/g}$. The profiles of the chosen seven possible sources were obtained from literature. The CMB model relies on the assumption that no change in source profile occurs between source and receptor. However, the researchers suggested that this assumption does not always hold, since differential loss of PAHs could be incurred from source to receptor as a result of photo-oxidation in the atmosphere, or photolysis, or biodegradation in the sediments. Consequently, the authors proposed a modification of the EPA CMB model by including degradation factors. After modifying the model for degradation factors, the model results indicated that diesel oil leaks (9.25 %), diesel engines exhaust (15.05 %), and coal burning (75.70 %) were the major sources of PAHs in sediments.

In a study carried out on sediments from the Green Bay, in Wisconsin, USA, coke burning, highway dust, and wood burning were found to be likely sources of PAHs [94]. The contribution of coke oven emissions for the Green Bay cores was in the range of 5–90 % while the overall highway dust contribution ranged between 5 and 70 %. This was determined after application of the CMB model. The authors did not take the possibility of degradation of the PAHs into account.

In another study, the sources of PAHs in sediments from the lower Fox River, Wisconsin, USA, were determined by applying the CMB model [86]. The sediment cores exhibited total PAH concentrations between 19.3 and 0.34 mg/kg. The researchers went a step further to determine historical trends of PAH inputs by employing ^{210}Pb and ^{137}Cs dating. Source fingerprints for CMB model input were obtained from literature. The results from the study indicated that coke oven emissions, highway dust, coal gasification, and wood burning were the likely sources of PAHs in the lower Fox River. Coke oven emissions were in the range of 40–90 % of total PAHs. Historical trend results revealed that this contribution decreased from 1930 to 1990. The overall highway dust contribution was between 10 and 75 %, and this fraction increased from 1930 to 2000. The wood burning contribution was less than 7 % in the cores.

The CMB model was employed to apportion sources of PAHs found in sediments from Lake Calumet and surrounding wetlands southeast of Chicago [91]. To establish the fingerprints of the PAH sources, 28 source profiles were obtained from literature. After taking into consideration gas/particle partitioning of some of the PAHs, some of the source profiles were modified accordingly. Modeling results indicated that coke ovens and traffic were the major sources of PAHs in the area. The average contribution from coke oven emissions ranged from 21 to 53 % of all sources, and that from traffic ranged from 27 to 63 %.

Duval and Friedlander used a CMB with first-order decay to resolve PAH sources to the Los Angeles atmosphere [95]. In this study, fingerprints of coal combustion (AN, PhA, FIA, Py, BaA, and chrysene), coke production (AN, PhA, BaP, BghiP), incineration (PhA, FIA, and especially Py), wood combustion (AN, PhA, FIA, and Py), oil burning (FIA and Py), gas-powered vehicles (FIA, Py, BghiP, and coronene), and diesel-powered vehicles (BbFIA, BkFIA, and thiophene compounds) were used to identify the sources. Subsequent application of the EPA CMB8.2 model quantified the contribution of each source.

A drawback of the CMB model is that *a priori* knowledge of the number of PAH sources is required. Coupled to this is the problem that location-specific profiles for PAH sources are not known. To ameliorate issues arising from the aforementioned problems, researchers have resorted to establishing the fingerprints of PAH sources, using data from the literature. Some of the source profiles are modified based on the gas/particle partitioning of individual PAHs. The profiles under the same source category are averaged, and the fingerprints of sources are established [91]. Although this approach has been used with some degree of success, the errors resulting from using source profiles from different regions or literature to represent local sources are not known. The profile reaching the receptor might be different from that at a source due to degradation processes occurring between source and receptor (Table 4).

Multivariate techniques

In contrast with the CMB, multivariate source apportionment methods require no *a priori* estimates of the number and compositions of components, for it searches for the data set for groups of species [such as principal components (PCs), factors, or clusters] whose collective variations account for most of the fluctuation of the species measured [82].

To date, PCA has been the most commonly used multivariate tool for PAH source apportionment and has been mainly applied for the purpose of identification. However, it is also possible to determine quantitatively the loading of each variable on each source, and the contribution of that source to the total pollutant concentration.

FA has been applied as a statistical technique to identify a relatively small number of factors (latent variables) that are used to represent the sources of contamination. Three common source apportionment techniques that are based on FA are: PMF, UNMIX, and PCA/MLR, which is also known as PCA/absolute principal component scores (PCA/APCS). Of these methods, PCA/MLR has been the technique most widely used for sediment studies.

PCA, FA, and MLR

PCA/MLR requires an initial PCA to be performed on the standardized data [96–98]. The PC matrix is then rotated using Varimax rotation, which retains the orthogonality of the axes and hence the independence of the latent variables (or sources) [34,97–99]. The rotation of the matrix realigns the matrix axes with the adjusted model parameters after the removal of the nonsignificant variables and thus clarifies the variable loading on each source [100]. Once this step has been completed, it is possible to identify the individual sources based on their chemical profiles. These chemical profiles may be defined variously by mathematical procedures [101], literature values [34,101–104], or diagnostic ratios [34,101–103,105].

The ultimate goal of source apportionment in environmental analysis is to determine the percentage contribution of different sources of pollutants for a given set of samples [105]. To achieve this goal, the percentage contributions of the major sources of pollutants are calculated using MLR from the PCA factor scores and the standardized normal deviation of total concentrations of pollutants as independent and dependent variables, respectively. The linear regression model was developed by Larsen and Baker [96]. The basic equation of a multiple linear model is

$$y = \sum m_i X_i + b \quad (6)$$

This model is only valid if the assumption that there is no collinearity in X_i holds. Noncollinearity, by definition, is ensured by selecting the PCA factor scores as the independent variables, X_i . The dependent variable, y , is Σ PAHs. The influence of each dependent variable on the independent variable can be directly compared by the regression coefficients, if the independent and dependent variables are “normally standardized”. The equation for normal standardization is

$$\text{standardized normal deviate of } x = (x - \bar{x})/\sigma_x \quad (7)$$

where x is any variable, \bar{x} is the mean of x , and σ_x is the standard deviation of x . This new variable represents the distance, in standard deviation units, of a given sample from the mean. When the variables of eq. 6 are normalized, the regression coefficients are represented as B , and the intercept (b) is 0

$$z = \sum B_i X_i \quad (8)$$

z becomes the standardized normal deviates of Σ PAHs. By definition, the factor scores have a mean of 0 and a standard deviation of 1; therefore, X_i after application of eq. 2 remains unchanged. The partial regression coefficient B_i is also the partial correlation coefficient, r_p , such that the squared multiple correlation coefficient, R^2 , can be expressed as

$$R^2 = \sum B_i^2 \quad (9)$$

The calculation of the mean percent contribution becomes

$$\text{mean contribution of source} = i(\%) = \frac{100B_i}{\sum B_i} \quad (10)$$

Most authors report the use of FA in combination with cluster analysis, and in all these cases the factor loadings are a reflection of the clustering of the PAHs. However, a few studies include MLR as part of the source apportionment strategy. In addition, these approaches have been employed to augment findings from other source apportionment approaches, such as CMBs.

One of the primary advantages of multivariate methodology, as applied to source apportionment, is the ability to include nonchemical measurements, such as light scattering, gaseous pollutant measurements, and meteorology in the data set. Thus, primary particles may be associated with secondary species. Another multivariate analysis strength is the ability to identify source impacts at the receptor with very limited knowledge of the airshed. The number of sources, likely emission composition and source loadings, are inferred directly from the data. In addition, these methods provide information concerning the number of major sources responsible for the data variability, source composition, and source loadings. These models, however, require large data sets and are, therefore, not useful for modeling single days. Finally, some knowledge of source compositions and sources likely to be impacting the receptor are required to interpret the model results (Table 4).

A drawback of PCA/MLRA is its inability to effectively model extreme data. This concept is an expression of the “nonrobustness” in the PCA/MLRA method (Table 4). In a study carried out by Larsen and Baker (2003) [96], 1-methylanthracene (1-MeA) had the highest loading on the wood source on a particular day. This PAH (1-MeA) also had the highest concentration on the day in question. These facts indicate that PCA created a factor to primarily account for the study, outlying 1-MeA concentration. A PCA/MLRA analysis was rerun without the data from the day in question, and a five-source solution was created. The factor loadings of the first four sources were similar to the original vehicle, coal, oil, and wood profiles. The fifth source was unidentifiable because of the lack of prominent chemical loadings. In the same study, approximately 10 % of the individual samples contained apparent negative source contributions; this is physically impossible. PCA’s ability to generate negative source contributions is a known major concern.

As a follow-up to the CMB model, an FA model with nonnegative constraints was employed to apportion the sources of PAHs found in sediments from Lake Calumet and surrounding wetlands southeast of Chicago [91]. The source profiles and contributions, with uncertainties, were determined with no prior knowledge of sources, as opposed to the CMB model where *a priori* knowledge of sources is a requirement (Table 4). The FA model included scaling, and back scaling, of data with average PAH concentrations, without normalization. The FA results for a two-source solution indicated coke oven (45 %) and traffic (55 %) as the primary PAH sources of Lake Calumet sediments. A six-source FA solution indicated that coke oven (47 %) and traffic (45 %) related sources were major PAH sources and wood burning-coal residential (2.3 %) was a minor PAH source. From the six-source solution, two coke oven profiles were observed, a standard coke oven profile (33 %), and a degraded or second coke oven profile (14 %), which was low in PhA and Py. Observed traffic-related sources included gasoline engine (36 %) exhaust and traffic tunnel air (9.3 %). These results augmented findings made using the CMB model.

The sources of PAHs that enter ambient air in Baltimore, MD, USA, were determined by using three source apportionment methods, PCA with MLR, EPA UNMIX model, and PMF [96]. In the study, vehicles with both diesel and gasoline engines contributed, on average, 16–26 %, coal 28–36 %, oil 15–23 %, and wood/other having the greatest disparity of 23–35 % of the total (gas-plus particle-phase) PAHs. Seasonal trends were found for both coal and oil. Coal was the dominant PAH source during the summer, while oil dominated during the winter. PMF was the only method to segregate diesel from gasoline sources. By determining the source apportionment through multiple techniques, weaknesses in individual methods were mitigated and overlapping conclusions were strengthened.

PCA and MLR were applied to apportion sources of PAHs in surface sediments in Tianjin River, China [106]. Four principal components were extracted representing coal combustion, petrol, coke and biomass burning, and industry discharge as sources. The contributions of major sources were quantified using MLR as 41 % coal, 20 % petroleum, and 39 % from coking and biomass. The researchers further divided the study area into three distinctive regions, with different PAH concentrations, and applied PCA and MLR to quantify contributions from major sources in those regions. The three zones were found to have distinctive differences in PAH concentration and profile, different source features were also unveiled. For the industrialized Tanggu-Hangu zone, the major contributors were coking (43 %),

coal (37 %), and vehicle exhausts (20 %). In rural areas, however, in addition to the three main sources, biomass burning was also important (13 %). In the urban–suburban zone, incineration accounted for one-fourth of the total.

The concentrations of 18 PAHs in 32 samples collected from the Huangpu River in Shanghai, China were determined [107]. Cluster analysis distinguished the 18 individual PAHs into three major groups. Two of the groups represented pyrogenic and petrogenic sources, while the third cluster represented an unknown source. The results of diagnostic ratios showed that pyrogenic sources were the major sources of the PAHs. The PCA/MLR analysis of the data revealed that contributions from coal combustion, traffic-related pollution, and spills of petroleum products (petrogenic) were 40, 36, and 24 %, respectively. Furthermore, the investigators were able to show that PAH pollution in the sediment was significantly higher in spring than in other seasons. They attributed the higher concentrations to contributions from coal combustion and petrogenic sources.

The PAHs in 350 sediments from a 2-km portion of the Little Menomonee River (Milwaukee, WI, USA) were determined using PCA, chemical fingerprinting, and PMF [45]. In total, creosote and urban background contributed 27 and 73 % of eight carcinogenic PAHs (CPAHs), respectively, in that part of the river. The concentrations of CPAHs derived from the urban background were highest in surface sediments (20 mg/kg), particularly near major roadway crossings. The concentration increased in the downstream direction, and (on average) exceeded the 15 mg/kg regulatory clean-up threshold. Weathered creosote-derived CPAHs were widespread at low concentrations (4.8 mg/kg), although some discrete sediments, mostly at depths below 2.54 cm, contained elevated CPAHs derived from creosote. The investigation demonstrated the value of combining multiple techniques in source apportionment studies of PAHs in sediments. Furthermore, it showed that PMF could be used as a means to determine the concentration of PAHs attributable to background in sediments without the need to identify, collect, and analyze background samples, which may not even exist in heterogeneous aquatic environments.

UNMIX and PMF

Efforts to develop other statistically driven source-receptor models that do not require prior knowledge of source profiles and are “robust” have been published. Two such models are the EPA UNMIX and PMF. UNMIX was developed to address the shortcomings of both PCA and CMBs [108]. Results from the UNMIX model are constrained to positive values, which address the most significant concern of PCA, i.e., sources which exhibit negative contributions. Unlike CMBs, UNMIX does not require *a priori* knowledge of the number of sources or their compositions (Table 4).

Given a data matrix of n samples with m chemical constituents, the model performs a singular value decomposition of the $n \times m$ matrix after it has been normalized such that all species have a mean of 1. This step reduces the dimensionality of the data space to the number of sources. Furthermore, UNMIX reduces the normalized source composition by projecting the data to a plane perpendicular to the first axis of N dimensional space. The boundaries or edges of the projected data represent the samples that characterize the sources. In contrast to PCA and other forms of source apportionment, UNMIX repeats the model calculations for each possible combination of m chemicals and retains only those constituents that contribute to improving the model’s signal-to-noise ratio [108].

In its simple form, the PMF equation can be written as

$$X = GF + E \quad (11)$$

where X = concentration data matrix for n number of samples and m chemical species; E = matrix of residuals; G = source contribution matrix for p sources and n number of samples, and F = source profile matrix for p sources and m chemical species. PMF resolves the receptor modeling problem by minimizing object function Q so that

$$Q = \sum_{i=1}^n \sum_{j=1}^m \left(\frac{e_{ij}}{s_{ij}} \right)^2 \quad (12)$$

where s_{ij} is the uncertainty in the j th chemical species in the i th sample and

$$e_{ij} = \gamma_{ij} - \sum_{k=1}^p g_{ik} f_{kj} \quad (13)$$

is the part of the data variance that was not explained by the model.

The principal objective of the application of PMF analysis to a data matrix with n number of samples and m number of chemical species is to resolve the number of p independent sources as well as the values of g_{ik} (source contribution) and f_{kj} (source profile) that best fit the concentration data, γ_{ij} . Thus, the number of pollutant sources and the contribution of each source to each sample obtained from a sampling site could be evaluated.

In addition to weighting the data points individually, PMF constrains the results to be always non-negative. This constraint reduces the rotational ambiguity in the FA problem with the view to obtaining physically realistic solutions. It also ensures that the outcomes are positive, since the concentrations of chemical species in environmental data cannot be negative [16].

Isotopic and molecular methods

The field of environmental forensics investigations pertaining to PAHs has recently benefited from the application of CSIA. Molecular analyses are often paired with CSIA when molecular signatures are inconclusive. CSIA has become an increasingly common and trusted analytical method for PAH source apportionment over the past 16 years. It exploits the isotopic rather than the molecular signature of PAH compounds, a signature that tends to be less subject to interference by weathering processes [109] (Table 4). O'Malley et al. [109] found that the isotope ratios of PAHs are not altered during processes such as volatilization, photolytic, and microbial degradation reactions (i.e., the isotopic signature of PAHs is conservative) [66]. These conditions make it possible to use isotopic fingerprints to implicate a source in the creation of PAHs because the fingerprint could be assumed to remain constant.

The main ratio of interest is that of ^{13}C to ^{12}C . This ratio is reported using delta notation, (eq. 1), which gives the per mil (‰) deviation of the isotope ratio of a sample from that of a standard

$$\delta^{13}\text{C}_{\text{sample}} = [({}^{13}\text{C}/{}^{12}\text{C})_{\text{sample}} / ({}^{13}\text{C}/{}^{12}\text{C})_{\text{standard}} - 1] \times 10^3 (\text{‰}, \text{VPDB}) \quad (14)$$

The Vienna Peedee belemnite (VPDB) standard has been the most commonly used for this type of analysis [110,111]. The primary geochemical concept on which CSIA is premised involves kinetic isotope effects. These effects determine which isotopes are preferentially incorporated into PAHs during formation or into their organic precursors during photosynthesis. Kinetic effects alter the isotope ratios of the resulting PAHs at each major stage and pathway to formation.

Isotope measurements of individual PAHs have been carried out using GS-isotope ratio mass spectrometry (IRMS) (Fig. 1) [109,112]. These specialized measurements have been conducted by using a GC coupled to an isotope-ratio magnetic sector mass spectrometer. The GC separates organic

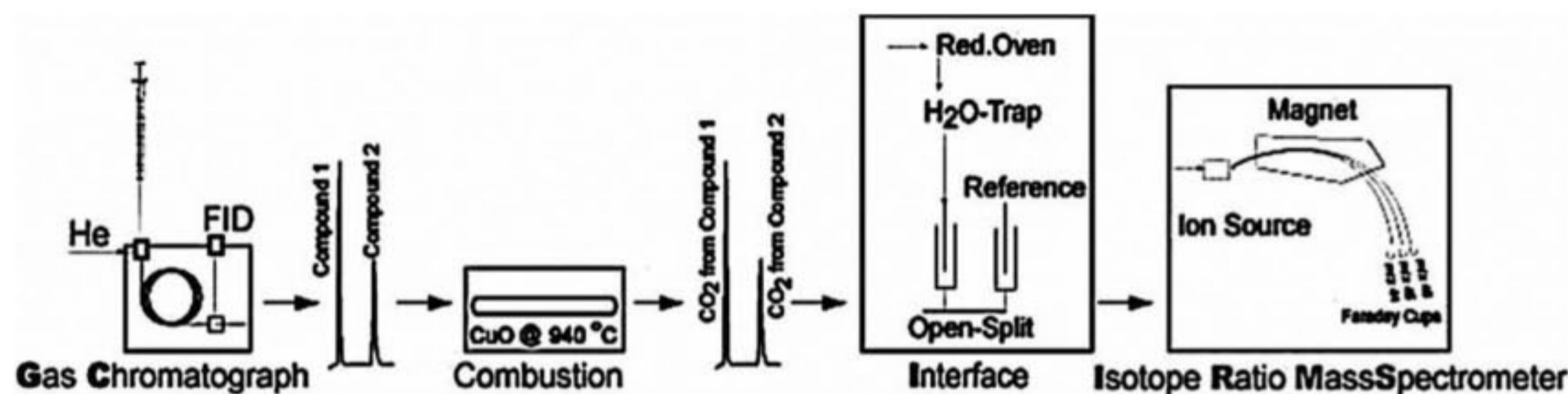


Fig. 1 Schematic diagram of GC/IRMS for $\delta^{13}\text{C}$ measurements [112].

components from one another in complex mixtures and is attached to a combustion furnace which converts organic components into CO₂. The CO₂ will have a mass of 45 or 44 depending on whether it contains ¹³C or ¹²C. The CO₂ then passes continuously through an IRMS where the isotope ratios of the compounds are determined by comparison with the 45:44 mass-to-charge ratio of reference CO₂ [110–112].

Although the potential of using the ¹³C/¹²C isotope ratio measurements to source environmental PAHs has been demonstrated with great success, it is argued that the variation in isotopic signatures within a range of only a few ‰ for different sources, may limit its use in resolving PAHs in some complex environments (Table 4). To improve on the differentiation of PAHs derived from petrol, jet fuel, and different coal conversion processes, Sun et al. [113] recommended the application of ¹³C values in conjunction with reported hydrogen stable isotopes D values. This is possible because deuterium enrichment takes place simultaneously with ¹³C depletion, which occurs during the formation of PAHs. The isotopic compositions of different petroleum products will vary from one another because they originate from different sources of crude oil. The δ¹³C and δ²H values used for differentiation of coal tar, jet fuel, and gasoline PAH sources are shown in Tables 5 and 6.

Table 5 δ¹³C isotopic ratios for PAHs from selected products of combustion [113].

| PAH | Gasworks coal tar | HT coal tar | Jet fuel | Gasoline |
|---------------------------------|----------------------|----------------|-------------|----------|
| Phenanthrene | -27.5 | -24.8 | -22.7 | -26.5 |
| Anthracene | -27.5 | -24.8 | -22.7 | -26.5 |
| Fluoranthene | -28.5 | -24.5 | -23.5 | -27.1 |
| Pyrene | -28.3 | -24.5 | -23.2 | -26.9 |
| Benzo[<i>a</i>]anthracene | -28.9 | -24.2 | -24.1 | -27 |
| Chrysene | -28.9 | -24.2 | -23.5 | -27 |
| Benzo[<i>b</i>]fluoranthene | -28.8 | -24.8 | -25.7 | -27.8 |
| Benzo[<i>k</i>]fluoranthene | -28.8 | -24.8 | -25.7 | -27.8 |
| Benzo[<i>a</i>]pyrene | -28.9 | -25.2 | -25.5 | -28.5 |
| Indeno[1,2,3- <i>cd</i>]pyrene | -29.5 | -26.4 | -27.8 | -29.4 |
| Dibenz[<i>a,h</i>]anthracene | -29.5 | -26.4 | -27.8 | -29.4 |
| Benzo[<i>ghi</i>]perylene | -30 | -26.6 | -28.1 | -29.6 |

Table 6 δ²H isotopic ratios for PAHs from selected products of combustion [113].

| PAH | Gasworks coal tar | HT coal tar | Jet fuel | Gasoline |
|---------------------------------|----------------------|----------------|-------------|----------|
| Phenanthrene | -49.3 | -73.2 | | -61.5 |
| Anthracene | -49.3 | | | -61.5 |
| Fluoranthene | -42.2 | -67.9 | -74.3 | -49.1 |
| Pyrene | -40 | -65.3 | -74.1 | -54.7 |
| Benzo[<i>a</i>]anthracene | -38.7 | -72.1 | -71.1 | -47.1 |
| Chrysene | -33.5 | -72.6 | -71.1 | -47.1 |
| Benzo[<i>b</i>]fluoranthene | -33.5 | -81.1 | -61.2 | -47 |
| Benzo[<i>k</i>]fluoranthene | -34 | -81.1 | -61.2 | -47 |
| Benzo[<i>a</i>]pyrene | -33.2 | -68.3 | -60.2 | -51.2 |
| Indeno[1,2,3- <i>cd</i>]pyrene | -33.2 | -75.5 | -68.9 | -49.2 |
| Dibenz[<i>a,h</i>]anthracene | -33.2 | | -68.9 | -51.2 |
| Benzo[<i>ghi</i>]perylene | -33.2 | -71.6 | -67.5 | -54 |

The potential of CSIA as a source apportionment technique was demonstrated by O'Malley et al. when they differentiated isotopic signatures of PAHs emitted by wood burning and those found in car soot [109]. The researchers noted that LMW PAHs tend to be enriched in ^{13}C and are characteristic of pyrogenic mixtures, while HMW PAHs depleted in ^{13}C were characteristic of petrogenic mixtures. In another study by McRae et al. [114], the utility of CSIA was demonstrated when PAHs generated by coal and biomass pyrolysis, and in diesel particulates, were found to possess substantially different isotopic signatures. These three sources could not, previously, be resolved without employing CSIA.

The technique CSIA was employed to apportion PAHs in sediments from St. John's Harbor in Newfoundland. The primary source was observed to be wood burning, instead of crankcase oil or other petrogenic sources [109]. In another study, chemical fingerprinting through molecular methods apportioned PAHs in an urban estuary in Virginia to wood-treatment facilities. However, application of isotope signature analysis revealed an additional source as coal transport [115].

To elucidate the various reaction mechanisms involved in the formation of PAHs by different sources, researchers have resorted to ^{13}C isotope measurements in products and sources. In one study it was observed that PAHs formed from different coal conversion processes could be differentiated with PAHs enriched in ^{12}C having a propensity to be preferentially formed at higher temperatures [110].

Despite the growing popularity of CSIA as a source apportionment technique for PAHs, the technique has some drawbacks. There is currently a lack of standardized methods for CSIA with respect to PAHs. Purification procedures, necessary to separate the aliphatic fraction from the PAH fraction because the two would otherwise coelute during GC-C-IRMS analysis, are continuously being modified and are inconsistent across studies [115]. Purification procedures have been cited as a reason why two studies differed in their attempt to apportion PAHs from creosote wood preservatives [114].

Although GC-C-IRMS is a fairly sensitive technique, relatively high detection limits of about 10 mg/L for an individual PAH, for each injected sample, often present challenges for analysis of natural samples. Some developments to circumvent this problem include large volume temperature-programmable injection method for GC-C-IRMS analysis of PAHs, which measures samples with concentrations as low as 0.07 mg/L [110]. This technique has superior sensitivity than the more common splitless injection approach.

Although the literature is awash with ^{13}C values for pyrogenic compounds, this has been at the expense of two other useful source apportionment ratios, i.e., ^{13}C values for petrogenic PAHs [71] and PAH δD values [116]. Sun et al. [113] revealed that analyzing PAH δD values in combination with ^{13}C values appears to be a promising strategy for differentiating similar sources. This is an area where future research should be focused to further expand the potential of CSIA as an environmental forensics tool.

CONCLUSIONS

PAH diagnostic ratios should be used with caution, as their values may be altered during the transport of these compounds to sediments. Their use should therefore be accompanied by the application of correction factors which partially take into consideration changes due to phase transport and degradation. In addition, the confidence in diagnostic ratios in source apportionment could be considerably improved by estimating PAH emission profiles for suspected emission sources present in the area to be investigated. To some extent, this prevents misinterpretations due to wrong assumptions of diagnostic ratios for particular sources. More than one diagnostic ratio should be used to confirm the results. The FIA/(FIA + Py) and IP/(IP + BghiP) ratios are more conservative than AN/(AN + PhA) and BaA/(BaA + Chy), which are particularly sensitive to photodegradation. The AN/(AN + PhA) ratio is sensitive to environmental changes, and its values for the identification of particular processes lie within a narrow range, which makes it hard to use.

Source apportionment of PAHs could be achieved through various other approaches which include receptor modeling and the use of isotope signatures. However, when these techniques are applied together more useful information is obtained. Multivariate approaches can yield both quantita-

tive and qualitative information. However, with PCA/MLR the robustness of this approach is compromised in cases where a PAH has high concentration leading to high factor loadings, thus introducing bias in the source apportionment. The PCA approach yields sources with negative contributions, which is not practical. The CMB model on the other hand requires *a priori* knowledge of sources. To circumvent these problems, the use of alternative statistically driven approaches such as PMF and UNMIX is prudent.

CSIA studies appear to have made a significant impact in the field of environmental forensics, though there are still areas of further research such as improving ^{13}C values for petrogenic PAHs and PAH δD values. Often, neither CSIA nor fingerprinting alone are conclusive for source apportionment, but the information gained from isotopic analysis will certainly make CSIA indispensable in future source allocation investigations.

REFERENCES

1. A. Amit, A. Taneja. *Chemosphere* **65**, 449 (2006).
2. G. Grimmer, J. Jacob, K. W. Naujack, G. Detbarn. *Anal. Chem.* **55**, 892 (1983).
3. U. Varanasi, J. E. Stein. *Environ. Health Perspect.* **90**, 93 (1991).
4. J. E. Stein, T. K. Collier, W. L. Reichert, E. Casillas, T. Hom, U. Varanasi. *Environ. Toxicol. Chem.* **11**, 701 (1992).
5. E. Cavalieri, E. Rogan. *Environ. Health Perspect.* **64**, 69 (1985).
6. M. P. Zakaria, H. Takada, S. Tsutsumi, K. Ohno, J. Yamada, E. Kouno, H. Kumata. *Environ. Sci. Technol.* **36**, 1907 (2002).
7. X. Liu, T. Korenaga. *J. Health Sci.* **47**, 446 (2001).
8. F. Sun, D. Littlejohn, M. David Gibson. *Anal. Chim. Acta* **364**, 1 (1998).
9. D. Mackay, W. Y. Shiu, K. C. Ma, S. C. Lee. *Handbook of Physical-Chemical Properties and Environmental Fate for Organic Chemicals*, p. 71, CRC Press, New York (2006).
10. A. Masih, A. Taneja. *Chemosphere* **65**, 449 (2006).
11. H. M. Hwang, T. L. Wade, J. L. Sericano. *Atmos. Environ.* **37**, 2259 (2003).
12. M. Tobiszewski, J. Namieśnik. *Environ. Pollut.* **162**, 110 (2012).
13. M. Odabasi, E. Cetin, A. Sofuoglu. *Atmos. Environ.* **40**, 6615 (2006).
14. Z. Wang, K. Li, P. Lambert, C. Yang. *J. Chromatogr., A* **1139**, 14 (2007).
15. H. J. Costa, T. C. Sauer. *Environ. Forensics* **6**, 9 (2005).
16. M. M. R. Mostert, G. A. Ayoko, S. Kokot. *Trends Anal. Chem.* **29**, 430 (2010).
17. J. Albaiges, B. Morales-Nin, F. Vilas. *Mar. Pollut. Bull.* **53**, 205 (2006).
18. J. W. Short, G. V. Irvine, D. H. Mann, J. M. Maselko, J. J. Pella, M. R. Lindeberg. *Environ. Sci. Technol.* **41**, 1245 (2007).
19. S. A. Stout, S. Emsbo-Mattingly. *Org. Geochem.* **39**, 801 (2008).
20. R. Booth, K. Gribben. *Environ. Forensics* **6**, 133 (2005).
21. S. Almaula. *Environ. Forensics* **6**, 143 (2005).
22. M. J. Ahrens, D. J. Morrissey. *Oceanogr. Mar. Biol. Ann. Rev.* **43**, 69 (2005).
23. H. Willsch, M. Radke. *Polycyclic Aromat. Compd.* **7**, 231 (1995).
24. P. W. French. *Environ. Pollut.* **103**, 37 (1998).
25. R. Johnson, R. M. Bustin. *Int. J. Coal Geol.* **68**, 57 (2006).
26. C. Pies, Y. Yang, T. Hofmann. *J. Soils Sediments* **7**, 216 (2007).
27. A. Koziol, J. Pudykiewicz. *Chemosphere* **45**, 1181 (2001).
28. F. Wania, D. Mackay. *Environ. Sci. Technol.* **30**, 390A (1996).
29. Y. Liu, L. Chen, Q. Huang, W. Li, Y. Tang, J. Zhao. *Sci. Total Environ.* **407**, 2931 (2009).
30. E. Galarneau. *Atmos. Environ.* **42**, 8139 (2008).
31. A. Katsoyiannis, E. Terzi, Q.-Y. Cai. *Chemosphere* **69**, 1337 (2007).

32. X. L. Zhang, S. Tao, W. X. Liu, Y. Yang, Q. Zuo, S. Z. Liu. *Environ. Sci. Technol.* **39**, 9109 (2005).
33. G. Gordon. *Environ. Sci. Technol.* **22**, 1132 (1988).
34. G. C. Fang, C. N. Chang, Y.-S. Wu, P. P. C. Fu, I. L. Yang, M. H. Chen. *Sci. Total Environ.* **327**, 135 (2004).
35. X. J. Wang, R. M. Liu, K. Y. Wang, J. D. Hu, Y. B. Ye, S. C. Zhang, F. L. Xu, S. Tao. *Environ. Geol.* **49**, 1208 (2006).
36. X. Q. Wang, M. Wang, H. L. Ge, Q. Chen, Y. B. Xu. *Physica E* **30**, 101 (2005).
37. A. Navarro, R. Tauler, S. Lacorte, D. Barceló. *Anal. Bioanal. Chem.* **385**, 1020 (2006).
38. K. Sielaff, J. Einax. *J. Soils Sediments* **7**, 45 (2007).
39. A. Facchinelli, E. Sacchi, L. Mallen. *Environ. Pollut.* **114**, 313 (2001).
40. S. Kokot, M. Grigg, H. Panayiotou, T. D. Phuong. *Electroanalysis* **10**, 1081 (1998).
41. X. Z. Yu, Y. Gao, S. C. Wu, H. B. Zhang, K. C. Cheung, M. H. Wong. *Chemosphere* **65**, 1500 (2006).
42. S. Stout, A. D. Uhler, K. J. McCarthy. "Chemical fingerprinting of hydrocarbons", in *Introduction to Environmental Forensics*, p. 147, Academic Press, New York (2001).
43. K. J. Emsbo-Mattingly, S. A. Stout, A. D. Uhler, G. S. Douglas, K. J. McCarthy, A. Coleman. *Land Contam. Reclam.* **14**, 403 (2006).
44. S. A. Stout, T. P. Graan. *Environ. Sci. Technol.* **44**, 2932 (2010).
45. H. Budzinski, I. Jones, J. Bellocq, C. Piérard, P. Garrigues. *Mar. Chem.* **58**, 85 (1997).
46. R. M. Dickhut, E. A. Canuel, K. E. Gustafson, K. Liu, K. M. Arzayus, S. E. Walker, G. Edgecombe, M. O. Gaylor, E. H. MacDonald. *Environ. Sci. Technol.* **34**, 4635 (2000).
47. A. Stark, T. Abrajano Jr., J. Hellou, J. L. Metcalf-Smith. *Org. Geochem.* **34**, 225 (2003).
48. S. E. Walker, R. M. Dickhut, C. Chisholm-Brause, S. Sylva, C. M. Reddy. *Org. Geochem.* **36**, 619 (2005).
49. B. Yan, T. A. Abrajano, R. F. Bopp, L. A. Benedict, D. A. Chaky, E. Perry, J. Song, D. P. Keane. *Org. Geochem.* **37**, 674 (2006).
50. B. Yan, T. A. Abrajano, R. F. Bopp, D. A. Chaky, L. A. Benedict, S. N. Chillrud. *Environ. Sci. Technol.* **39**, 7012 (2005).
51. M. B. Yunker, R. W. Macdonald, R. Brewer, S. Sylvestre, T. Tuominen, M. Sekela, R. H. Mitchell, D. W. Paton, B. R. Fowler, C. Gray, D. Goyette, D. Sullivan. *Assessment of Natural and Anthropogenic Inputs Using PAHs as Tracers. The Fraser River Basin and Strait of Georgia 1987–1997*, U.S. Environmental Protection Agency (Ed.), pp. 36–47, EPA, Washington, DC (2000).
52. M. B. Yunker, R. E. Macdonald. *Arctic* **48**, 118 (1995).
53. B. D. McVeety, R. A. Hites. *Atmos. Environ.* **22**, 511 (1988).
54. U. Ghosh, S. B. Hawthorne. *Environ. Sci. Technol.* **44**, 1204 (2010).
55. D. S. Page, P. D. Behm, G. S. Douglas, A. E. Bence, W. A. Burns, P. Mankiewicz. *Mar. Pollut. Bull.* **38**, 247 (1999).
56. X. C. Wang, S. Sun, H. Q. Ma, Y. Liu. *Mar. Pollut. Bull.* **52**, 129 (2006).
57. V. Rocher, S. Azimi, R. Moilleron, G. Chebbo. *Sci. Total Environ.* **323**, 107 (2004).
58. G. Li, X. Xia, Z. Yang, R. Wang, N. Voulvoulis. *Environ. Pollut.* **144**, 985 (2006).
59. Z. Zhang, J. Huang, G. Yu, H. Hong. *Environ. Pollut.* **130**, 249 (2004).
60. Y. Lang, Z. Cao. In *Bioinformatics and Biomedical Engineering (iCBBE), 2010 4th International Conference on*, p. 1 (2010).
61. Z. Guo, T. Lin, G. Zhang, Z. Yang, M. Fang. *Environ. Sci. Technol.* **40**, 5304 (2006).
62. K. Ravindra, E. Wauters, R. Van Grieken. *Sci. Total Environ.* **396**, 100 (2008).
63. M. S. Callén, M. T. Cruz, J. M. López, A. M. Mastral. *Fuel Process. Technol.* **92**, 176 (2011).
64. G. Li, X. Xia, Z. Yang, R. Wang, N. Voulvoulis. *Environ. Pollut.* **144**, 985 (2006).

65. H. H. Soclo, P. Garrigues, M. Ewald. *Mar. Pollut. Bull.* **40**, 387 (2000).
66. M. P. Zakaria, H. Takada, S. Tsutsumi, K. Ohno, J. Yamada, E. Kouno, H. Kumata. *Environ. Sci. Technol.* **36**, 1907 (2002).
67. M. Ricking, H. M. Schulz. *Mar. Pollut. Bull.* **44**, 565 (2002).
68. Y. Liu, L. Chen, Z. Jianfu, H. Qinghui, Z. Zhiliang, G. Hongwen. *Environ. Pollut.* **154**, 298 (2008).
69. X. J. Luo, S. J. Chen, B. Mai, G. Sheng. *Arch. Environ. Contam. Toxicol.* **55**, 11 (2008).
70. A. Wagener, C. Hamacher, C. Farias, J. M. Godoy, A. Scofield. *Mar. Chem.* **121**, 67 (2010).
71. J. W. Readman, R. F. Mantoura, M. M. Rhead. *Sci. Total Environ.* **66**, 73 (1987).
72. B. D. McVeety, R. A. Hites. *Atmos. Environ.* **22**, 511 (1988).
73. M. B. Yunker, R. W. Macdonald, R. Vingarzan, R. H. Mitchell, D. Goyette, S. Sylvestre. *Org. Geochem.* **33**, 489 (2002).
74. D. Mackay, W. Y. Shiu, K. C. Ma, S. C. Lee. *Handbook of Physical-Chemical Properties and Environmental Fate for Organic Chemicals*, p. 58, CRC Press, New York (2006).
75. P. Masclat, G. Mouvier, K. Nikolaou. *Atmos. Environ.* **20**, 439 (1986).
76. R. M. Kamens, Z. Guo, J. N. Fulcher, D. A. Bell. *Environ. Sci. Technol.* **22**, 103 (1988).
77. T. D. Behymer, R. A. Hites. *Environ. Sci. Technol.* **22**, 1311 (1988).
78. A. Li, J.-K. Jang, P. A. Scheff. *Environ. Sci. Technol.* **37**, 2958 (2003).
79. M. P. Fraser, G. R. Cass, B. R. Simoneit, R. A. Rasmussen. *Environ. Sci. Technol.* **32**, 1760 (1998).
80. E. Manoli, A. Kouras, C. Samara. *Chemosphere* **56**, 867 (2004).
81. T. Nielsen. *Atmos. Environ.* **22**, 2249 (1988).
82. G. Gordon. *Environ. Sci. Technol.* **22**, 1132 (1988).
83. R. C. Henry, C. W. Lewis, P. K. Hopke, H. J. Williamson. *Atmos. Environ. (1967)* **18**, 1507 (1984).
84. S. K. Friedlander. *Environ. Sci. Technol.* **7**, 235 (1973).
85. L. Xue, Y. Lang, A. Liu, J. Liu. *Environ. Monit. Assess.* **163**, 57 (2010).
86. M. C. Su, E. R. Christensen, J. F. Karls, S. Kosuru, I. Imamoglu. *Environ. Toxicol. Chem.* **19**, 1481 (2000).
87. K. Li, E. R. Christensen, R. P. V. Gamp, I. Imamoglu. *Environ. Sci. Technol.* **35**, 2896 (2001).
88. A. Miguel, P. Pereira. *Aerosol Sci. Technol.* **10**, 292 (1989).
89. K. Sexton, K. Liu, S. Hayward, J. Spengler. *Atmos. Environ.* **19**, 1225 (1985).
90. EPA. *Chemical Mass Model (EPA-CMB8.2)*, U.S. Environmental Protection Agency, Washington, DC (2009).
91. A. Li, J. K. Jang, P. A. Scheff. *Environ. Sci. Technol.* **37**, 2958 (2003).
92. G. M. Hidy, C. Venkataraman. *Chem. Eng. Commun.* **151**, 187 (1996).
93. J. G. Watson. *JAPCA* **34**, 619 (1984).
94. M. C. Su, E. R. Christensen, J. F. Karls. *Environ. Pollut.* **99**, 411 (1998).
95. M. M. Duval, S. K. Friedlander. *Source Resolution of Polycyclic Aromatic Hydrocarbons in the Los Angeles Atmospheres Application of a CMB with First Order Decay*, U.S. Environmental Protection Agency, Washington, DC (1981).
96. R. I. Larsen, J. Baker. *Environ. Sci. Technol.* **37**, 1873 (2003).
97. M. F. Simcik, S. J. Eisenreich, P. J. Liroy. *Atmos. Environ.* **33**, 5071 (1999).
98. G. D. Thurston, J. D. Spengler. *J. Climate Appl. Meteorol.* **24**, 1245 (1985).
99. K. P. Singh, A. Malik, R. Kumar, P. Saxena, S. Sinha. *Environ. Monit. Assess.* **136**, 183 (2007).
100. C. Zhang, L. Wu, Y. Luo, H. Zhang, P. Christie. *Environ. Pollut.* **151**, 470 (2008).
101. R. C. Brandli, T. D. Bucheli, S. Ammann, A. Desaulles, A. Keller, F. Blum, W. A. Stahel. *J. Environ. Monit.* **10**, 1278 (2008).
102. N. R. Khalili, P. A. Scheff, T. M. Holsen. *Atmos. Environ.* **29**, 533 (1995).

103. E. Manoli, D. Voutsas, C. Samara. *Atmos. Environ.* **36**, 949 (2002).
104. R. M. Harrison, D. J. T. Smith, L. Luhana. *Environ. Sci. Technol.* **30**, 825 (1996).
105. P. Fernandez, R. M. Vilanova, J. O. Grimalt. *Environ. Sci. Technol.* **33**, 3716 (1999).
106. Q. Zuo, Y. H. Duan, Y. Yang, X. J. Wang, S. Tao. *Environ. Pollut.* **147**, 303 (2007).
107. Y. Liu, L. Chen, Q. Huang, W. Li, Y. Tang, J. Zhao. *Sci. Total Environ.* **407**, 2931 (2009).
108. R. Henry, C. Lewis, J. Collins. *Environ. Sci. Technol.* **28**, 823 (1994).
109. D. Kim. *Chemosphere* **76**, 1075 (2009).
110. V. P. O'Malley, T. A. Abrajano, J. Hellou. *Org. Geochem.* **21**, 809 (1994).
111. V. P. O'Malley, T. A. Abrajano, J. Hellou. *Environ. Sci. Technol.* **30**, 634 (1996).
112. V. P. O'Malley, R. A. Burke, W. S. Schlotzhauer. *Org. Geochem.* **27**, 567 (1997).
113. C. Sun, M. Cooper, C. E. Snape. *Rapid Commun. Mass Spectrom.* **17**, 2611 (2003).
114. C. McRae. *Anal. Commun.* **33**, 331 (1996).
115. S. E. Walker. *Org. Geochem.* **36**, 619 (2005).
116. T. Okuda, H. Kumata, H. Naraoka, H. Takada. *Org. Geochem.* **33**, 1737 (2002).